Research Article Vol. 60, No. 15 / 20 May 2021 / Applied Optics 4291

applied optics

Efficiency analysis of cellular/LiFi traffic offloading

Haitham S. Khallaf,[1,*] Abd El-Rahman A. El-Fikky,[2] Mohamed Elwekeil,[3] Abdulaziz E. Elfiqi,[3] Ehab Mahmoud Mohamed,[4,5] and Hossam M. H. Shalaby[2,6]

[1]Nuclear Research Center, Egyptian Atomic Energy Authority (EAEA), Inshas 13759, Egypt
[2]Electrical Engineering Department, Faculty of Engineering, Alexandria University, Alexandria 21544, Egypt
[3]Department of Electronics and Electrical Communications Engineering, Faculty of Electronic Engineering (FEE), Menoufia University, Menouf 32952, Egypt
[4]College of Engineering, Prince Sattam Bin Abdulaziz University, Wadi Aldwaser 11991, Saudi Arabia
[5]Electrical Engineering Department, Faculty of Engineering, Aswan University, Aswan 81542, Egypt
[6]Department of Electronics and Communications Engineering, Egypt-Japan University of Science and Technology (E-JUST), Alexandria 21934, Egypt
*Corresponding author: eng.h.khallaf@gmail.com

Received 14 January 2021; revised 20 April 2021; accepted 20 April 2021; posted 21 April 2021 (Doc. ID 419593); published 13 May 2021

Data offloading is a promising low-cost and power-efficient solution for the expected high demands for high-speed connectivity in the near future. We investigate offloading efficiency in a cellular/light fidelity (LiFi) network. This offloading efficiency is a measure of the ratio of traffic carried by the LiFi network to the total traffic carried by both LiFi and cellular networks. We consider the two scenarios of opportunistic and delayed offloading. Effects of user density, user mobility, LiFi-signal blocking, and channel characteristics are investigated. We use Zemax to simulate LiFi channels in the proposed model. Based on our results, delayed offloading can achieve up to 60% offloading efficiency while opportunistic offloading achieves up to 18% offloading efficiency.

https://doi.org/10.1364/AO.419593

1. INTRODUCTION

Based on Cisco's study about global mobile traffic introduced in [1], traffic will increase by sevenfold from 2016 to 2021, internet clients will increase by 36% in 2023 compared to 2018, and the number of devices connected to IP networks will be more than 3 times the global population by 2023. These expected high demands for connectivity motivated researchers in both academic and industry to introduce cost-effective and power-saving solutions, for example, employing higher frequencies to offload traffic from cellular systems and increasing the spectral efficiency by using massive multiple-input multiple-output (MIMO) [2–4]. Using wireless fidelity (Wi-Fi) and mm wave technologies to offload cellular systems has been investigated widely in literature [5–9].

Recently, visible light communication (VLC), also known as light fidelity (LiFi), has been introduced as a new tier in heterogeneous networks (HetNets) [10]. VLC has advantages over radio frequency (RF) communications, e.g., wide-free frequency spectrum, low transmitted power, low cost, easy installation, fewer health problems related to VLC transmitted power, and security of communication [11–13]. Using WiFi and LiFi in fifth generation (5G) mobile networks has been discussed in [14]. The authors have introduced several ways of channel aggregation for the suggested coexistence. In [14], proof-of-concept results are presented through LiFi and WiFi front-ends. Specifically, it has been reported that both technologies can foster each other to provide more than 3 times the individual user's throughput, offer significant synergy, enhance the indoor coverage, and increase the peak data rates required by 5G network applications [14].

Channel modeling is an essential part in communication system design and performance optimization [15–17]. VLC static channel models have been considered in [18,19]. However, these models did not include shadowing effects resulted from mobility of both user of the VLC equipment and surrounding people. Dynamic channel models have been introduced in [20–23]. In [20], the effect of user mobility on VLC channel gain variations is experimentally calculated by modeling human bodies as box-shaped objects. Random motions in [20] have been done by moving these boxes manually. The authors revealed that Rayleigh distribution achieves good fitting according to their measurements for the channel gain. The dynamic VLC channel modeling has been investigated in [21] where it has been shown that Weibul, log-normal, and Nakagami fit results for single-input single-output (SISO) and single-input multiple-output (SIMO) models in the case of good channel conditions. In [22], both Nakagami and log-normal channels have been studied in indoor dynamic channel modeling for the blockage time. The authors have proven the significant role of dynamic modeling

compared with static modeling in terms of bit error rate (BER) and outage probability.

Motivated by the inherent promising characteristics and the infrastructures availability of LiFi system, we work in this paper on analyzing the efficiency of using LiFi to offload data from cellular system. The main contributions in this paper are:

- We extend our work in [24] by including opportunistic and delayed offloading scenarios. We use the same strategy as that used in [9] to introduce analytical model to describe the operation of cellular/LiFi systems. However, channel characteristics of LiFi systems are different from WiFi systems. Thus, we need to introduce accurate channel model for dynamic VLC channel.
- This accurate channel model for dynamic LiFi system is obtained using Zemax Optic Studio simulator. We use accurate computer-aided designs (CADs) for human body and real coating materials for both human bodies and surrounding objects. In addition, we consider user mobility in the form of the random motion model.
- We analytically describe both opportunistic and delayed offloading scenarios and then evaluate offloading efficiencies in both scenarios using extensive Monte Carlo (MC) simulations.

The rest of this paper is organized as follows. In Section 2, state and timing diagrams for different offloading cases are explained. Mathematical expressions for the distributions of different timing parameters are given in Section 4. In Section 3, a Zemax Optic Studio simulator is used to simulate a dynamic VLC channel for different people densities. In Section 5, the LiFi offloading efficiency is investigated numerically. Finally, the conclusions are given in Section 6.

2. LIFI OFFLOADING SCENARIOS

We propose that the user equipment (UE) is covered by cellular system all the time, and when the UE is covered by LiFi, this UE offloads its traffic from cellular system by sending it over LiFi. Offloading techniques can be classified to two main types, namely, opportunistic and delayed offloading. In opportunistic offloading, the UE offloads data when LiFi is available, or else it keeps using cellular system while, in delayed offloading, if the UE has data to send, it waits some time with the expectation of connection to a LiFi access point (AP) before using cellular system. In the next sections, we explain state and timing diagrams for both opportunistic and delayed offloading scenarios. The definitions of the used time symbols are given in Table 1.

A. Opportunistic Offloading Scenario

The operations implemented during opportunistic cellular/LiFi offloading are described in the state diagram shown in Fig. 1(a). We suppose that the UE is covered by the cellular network all the duration, and the UE can be managed by either cellular or LiFi cells. When the session starts (SS), the UE scans if it is covered by a LiFi network or not. If there is an appropriate LiFi AP, the UE will be connected by this LiFi AP. Otherwise, the UE will be linked to the RF cellular network. During data transmission through cellular network, the UE keeps searching for LiFi coverage. If LiFi coverage is found, the UE will connect to the new LiFi AP. Under LiFi connection, when the LiFi reaches a signal level below a threshold level, a reverse vertical handover (RHO) from LiFi to cellular network occurs. Moreover, Fig. 1(b) reveals different timing cases for cellular/LiFi offloading.

Table 1. Different Timing Parameters of Cellular/LiFi Network

Parameter	Symbol
Cellular residence time	t_c
LiFi residence time	t_v
LiFi blocking time	t_b
Data rate over cellular cell	R_C
Data rate over LiFi cell	R_v
Expected session time	t_d
Elapsed time from session start to first vertical handover	t_r
A waiting time for searching LiFi network in delayed offloading	D

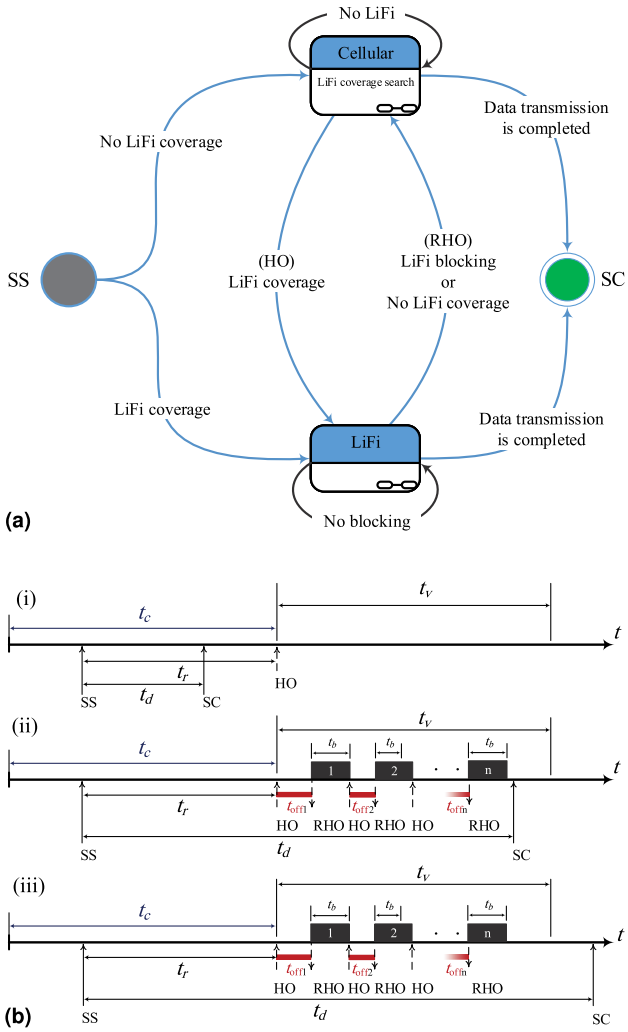

Fig. 1. (a) Traffic offloading state diagram of opportunistic cellular/LiFi HetNet: SS, session starts; SC, session completes; HO, vertical handover from cellular to LiFi cells; RHO, reverse vertical handover from LiFi to cellular cells. (b) LiFi offloading timing diagram for different cases: (i) $t_d < t_r$, (ii) $t_r \le t_d < t_r + t_v$, and (iii) $t_d \ge t_r + t_v$.

The average LiFi offloading times can be calculated from the average of three distinct cases:

1. When $t_d < t_r$, as shown in Fig. 1(b-i), no traffic is offloaded to LiFi network, and $E\{\sum t_{\text{off}}\} = 0$, with $E(\cdot)$ denoting the expectation operator.
2. When $t_r \le t_d < t_r + t_v$, as shown in Fig. 1(b-ii), the expectation of offloading time is given by $E\{\sum t_{\text{off}}\} = E\{t_d - t_r - \sum t_b\}$.
3. When $t_d \ge t_r + t_v$, as shown in Fig. 1(b-iii), the expectation of offloading time is given by $E\{\sum t_{\text{off}}\} = E\{t_v - \sum t_b\}$.

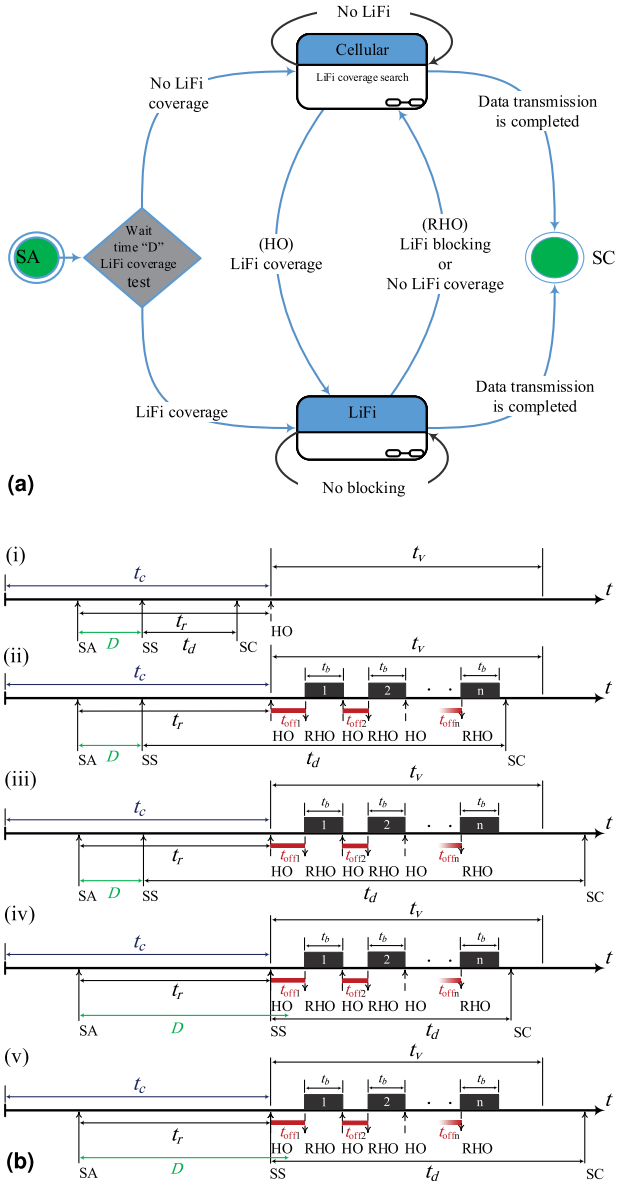

Fig. 2. (a) Traffic offloading of delayed cellular/LiFi HetNet state diagram: SA, start attempt; SS, session starts; SC, session completes; HO, vertical handover; RHO, reverse vertical handover. (b) LiFi offloading timing diagrams for various cases: (i) $D + t_d < t_r$, (ii) $D < t_r$ and $t_r \le t_d < t_r + t_v$, (iii) $D < t_r$ and $t_d \ge t_r + t_v$, (iv) $D > t_r$ and $t_r \le t_d < t_r + t_v$, and (v) $D > t_r$ and $t_d \ge t_r + t_v$.

B. Delayed Offloading Scenario

The operations implemented during delayed cellular/LiFi offloading are shown in Fig. 2(a). Similar to the opportunistic scenario, we consider that the UE can be served by the cellular network all the time, and this UE can connect to either cellular or LiFi networks. As long as the user attempts to make connection, start attempt (SA), and there is an available LiFi AP, the UE will be served by this LiFi AP and the SS. Otherwise the UE keeps looking for a LiFi AP during a wait time D before connecting to cellular systems. Through the data transmission through cellular network, the UE keeps searching for LiFi coverage. When the LiFi coverage is discovered, the UE will be linked to the new LiFi AP. In case the UE LiFi-signal level becomes below a threshold level, a RHO from LiFi to the cellular network will take place. The reason of signal degradation is due to the blocking of the light-signal.

Moreover, Fig. 2(b) shows different timing cases for cellular/LiFi delayed offloading. The average LiFi offloading times can be calculated from the average of five distinct cases:

1. When $D + t_d < t_r$, as shown in Fig. 2(b-i), no traffic is offloaded to LiFi network, and $E\{\sum t_{\text{off}}\} = 0$.
2. When $D < t_r$ & $t_r \le t_d < t_r + t_v$, as shown in Fig. 2(b-ii), the expectation of offloading time is given by $E\{\sum t_{\text{off}}\} = E\{t_d + D - t_r - \sum t_b\}$.
3. When $D < t_r$ and $t_d \ge t_r + t_v$, as shown in Fig. 2(b-iii), the expectation of offloading time is given by $E\{\sum t_{\text{off}}\} = E\{t_v - \sum t_b\}$.
4. When $D > t_r$ and $t_r \le t_d < t_r + t_v$, as shown in Fig. 2(b-iv), the expectation of offloading time is given by $E\{\sum t_{\text{off}}\} = E\{t_d - \sum t_b\}$.
5. When $D > t_r$ and $t_d \ge t_r + t_v$, as shown in Fig. 2(b-v), the expectation of offloading time is given by $E\{\sum t_{\text{off}}\} = E\{t_v - \sum t_b\}$.

3. VISIBLE LIGHT COMMUNICATIONS CHANNEL MODEL

Channel modeling is an essential part in the design of any communications system. Thus, in this section, we use Zemax Optics Studio, which is considered as a Monte Carlo ray tracing (MCRT) simulator, to obtain the VLC channel gain variations in a scenario of dynamic environment. We consider different mobile users densities, from one user up to nine users inside a standard office room of dimensions $5 \times 5 \times 3$ m^3, as shown in Fig. 3. Each mobile user in the room is equipped with a single UE that is able to communicate using VLC. The materials used for the ceiling, floor, and walls have a variable reflection coefficient that is wavelength dependent. Moreover, the coating for heads and hands are modeled as absorbing clothes and dark skin as configured in [22,25]. Additionally, we assume that objects are made of purely diffuse material, which is considered to be the worst scenario where the reflected rays may exhibit random angles compared with specular reflections. Moreover, we utilize advanced three-dimensional human CADs [26] and assume a real human's dimensions for height, width, and depth, which are 1.8, 0.4, and 0.2 m, respectively. The mobile users in the simulation are chosen according to the people density criteria

Fig. 3. Mobile users random mobility algorithm in an indoor dynamic VLC scenario for a standard room of dimensions $5 \times 5 \times 3\ m^3$.

Table 2. VLC Simulation Parameters Used in Zemax Optics Studio [19,22]

Link Parameter	Value
Size of room	$5 \times 5 \times 3\ m^3$
Lighting commercial Cree LEDs	4
Total chips per LED	100
Transmitted rays per chip	500,000 rays
Viewing angle of transmitter	120°
Area of rectangular photodiode	$1\ cm^2$
Configuration of reflection coefficients	Pure diffuse material
Field of view (FOV) of photodiode	85°
Power of each LED chip	0.45 W
Lighting positions	(1.5,1.5,2.85), (1.5,3.5,2.85), (3.5,1.5,2.85), (3.5,3.5,2.85)
Human reflection coefficient (maximum absorption)	0.1
Total reflections	7

> 0.16 people/m^2 to ensure the worst scenario conditions of fading as given in [20]. All simulation parameters used in the MCRT solver are given in Table 2.

The flow chart shown in Fig. 4 illustrates the complete simulation process. First, the number of users inside the room is decided, and random location and UE orientation are given for each of them. We assume users are moving in random motions inside the room with speeds following uniform distribution between 0.56 and 1.39 m/s and there are no random stops. The orientation of the UE is random and follows uniform distributions between 0° and 360°. In each iteration, users move random distance in a random direction, and new random UE orientation is generated for each user. We assume a safe distance of 1 m to avoid any collision between mobile users during movement, and the same distance is kept between the mobile users and the walls. Thus, we check these safe distances for each generated user's random displacement. If these conditions do not hold, we generate new random displacements. After that, we calculate the channel gain for that iteration using

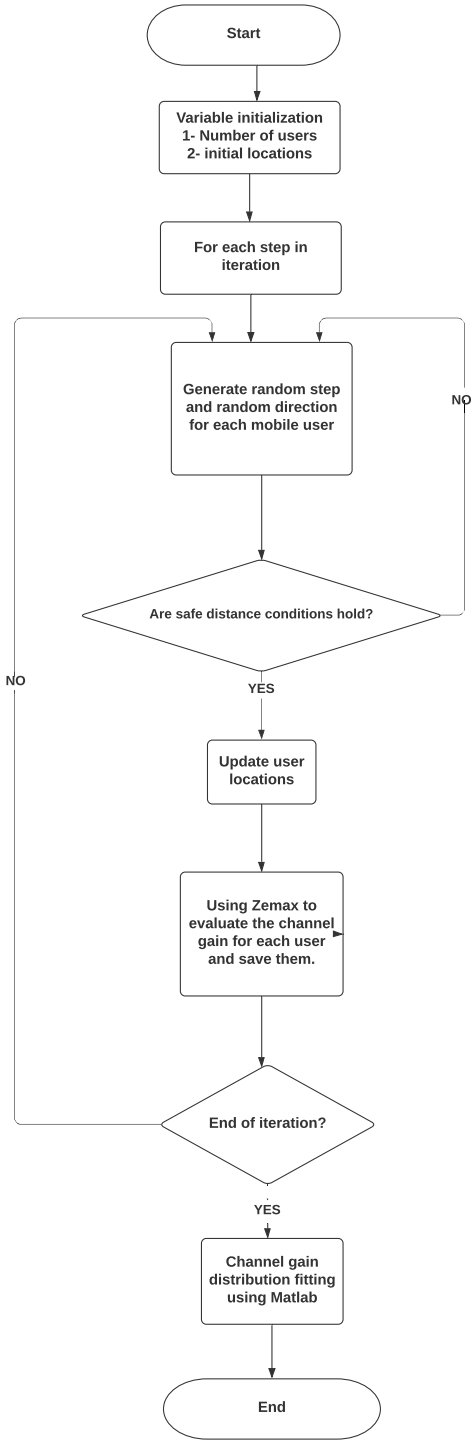

Fig. 4. Flow chart describing the whole simulation for the dynamic channel modeling.

Zemax Optics Studio. This process is repeated for 1000 iterations. We use Zemax Optics Studio with Zemax programming language (ZPL) [27] to be able to apply these 1000 iterations automatically rather than using one specific scenario like the static configuration. Then the channel gain results of the 1000 iterations are forwarded to MATLAB fit tool box to obtain the best fitting channel distribution.

Table 3. Resulted Rayleigh Parameter σ Values Versus People Densities from the Fit Tool Box in MATLAB

Mobile Users Densities	Rayleigh Distribution σ Value
1 mobile user	8.62719×10^{-5}
3 mobile users	7.93829×10^{-5}
5 mobile users	7.35083×10^{-5}
7 mobile users	6.94399×10^{-5}
9 mobile users	6.53201×10^{-5}

The channel impulse response used in the MCRT solver is specified by [19,22]

$$h(t) = \sum_{i=1}^{N_r} p_i \delta(t - \tau_i), \tag{1}$$

where p_i and τ_i are the power and delay for the ith ray, respectively, and N_r is the total number of rays emitted by the LEDs. Consequently, the channel DC gain H_0 is [19,22]

$$H_0 = \int_{-\infty}^{\infty} h(t)\mathrm{d}t. \tag{2}$$

The total received power at the receiver is defined by [21,22]

$$P_r = P_t H_d(0) + \int P_t H_{\mathrm{ref}}(0), \tag{3}$$

where $H_d(0)$ and $H_{\mathrm{ref}}(0)$ are the DC channel gains of the direct and reflected paths, respectively, and P_t is the total optical transmitted power by LEDs. The distribution fit toolbox in MATLAB is used to represent the statistical data and obtain the distribution parameters that best fit the data. The Rayleigh distribution proved satisfactory fitting with obtained results in the dynamic channel scenario. The results are listed in Table 3. As illustrated in that table, by increasing the people density, the parameter σ decreases. This reflects the effect of the shadowing due to people density, which cannot be neglected and should be taken into consideration.

4. OFFLOADING EFFICIENCY ANALYSIS

In this section, we analytically represent offloading efficiency, which expresses the ratio of the traffic that carried over a LiFi network to the total traffic over cellular/LiFi HetNet. Accordingly, offloading efficiency can be can be expressed as

$$\eta_{\mathrm{off.}} = \frac{R_v E\{t_{\mathrm{off}}\}}{R_v E\{\sum t_{\mathrm{off}}\} + R_C \left(E\{t_d\} - E\{\sum t_{\mathrm{off}}\}\right)}, \tag{4}$$

where R_v and R_C are the data rate over LiFi and cellular networks, respectively.

A. Statistical Distributions of Different Timing Parameters

In this section, we describe mathematical expressions for the distributions of different timing parameters, specifically cellular residence time (t_c), LiFi residence time (t_v), session time (t_d), elapsed time from SS to the first handover (t_r), and the blocking time (t_b).

The cellular residence time (t_c) follows a general distribution with mean μ_c^{-1} [28]. Besides, we consider exponential distribution with mean (μ_c^{-1}) to describe t_c with probability density function (pdf) $f_{t_c}(t_c; \mu_c)$ and cumulative distribution function (CDF) $F_{t_c}(t_c; \mu_c)$ given as

$$f_{t_c}(t_c; \mu_c) = \mu_c \exp(-\mu_c t_c), \tag{5}$$

$$F_{t_c}(t_c; \mu_c) = 1 - \exp(-\mu_c t_c). \tag{6}$$

Moreover, we consider the user-centric LiFi network: once a user finds LiFi coverage, the user stays a long time inside it. Based on that scenario, LiFi residence time (t_v) can be characterized by a two-stage hyper-exponential distribution with mean μ_v^{-1}. The corresponding pdf and CDF are given as [9,28]

$$f_{t_v}(t_v; \mu_v) = \frac{a^2}{a+1}\mu_v \exp(-a\mu_v t_v) + \frac{1/a}{a+1}\mu_v \exp\left(-\frac{\mu_v}{a}t_v\right), \tag{7}$$

$$F_{t_v}(t_v; \mu_v) = 1 - \frac{a}{a+1}\exp(-a\mu_v t_v) + \frac{1}{a+1}\exp\left(-\frac{\mu_v}{a}t_v\right), \tag{8}$$

respectively, where a is a variability parameter that affects the skewness of t_v. As a increases, $f_{t_v}(t_v; \mu_v)$ becomes more skewed to the left with a longer tail, i.e., the probability of shorter LiFi residence time increases [9]. The session time (t_d) follows an exponential distribution with mean μ_d^{-1}. The corresponding pdf and CDF are given as

$$f_{t_d}(t_d; \mu_d) = \mu_d \exp(-\mu_d t_d), \tag{9}$$

$$F_{t_d}(t_d; \mu_d) = 1 - \exp(-\mu_d t_d). \tag{10}$$

Based on the residual life theorem [9], the pdf of elapsed time from SS to the first handover (t_r) is defined as $f_{t_r}(t_r) = \mu_c(1 - F_{t_c}(t_r; \mu_c))$. Considering the distributions that describe t_c are exponential with mean μ_c^{-1}, then the pdf and CDF of t_r are given as follows [9]:

$$f_{t_r}(t_r; \mu_c) = \mu_c \exp(-\mu_c t_r), \tag{11}$$

$$F_{t_r}(t_r; \mu_c) = 1 - \exp(-\mu_c t_r). \tag{12}$$

The blocking time (t_b) is the time during which a user is covered by LiFi AP but the receiving power level is less than the specific threshold, Γ_{TH}. Thus, t_b is well described by a joint independent probability, and its CDF is given as follows:

$$F_{t_b}(t_b) = P_r(P < \Gamma_{\mathrm{TH}})\left[1 - F_{t_v}(t_b; \mu_v)\right] = \left[1 - \exp\left(-\frac{\Gamma_{\mathrm{TH}}}{2\sigma^2}\right)\right]\left[1 - F_{t_v}(t_b; \mu_v)\right]. \tag{13}$$

Based on our results in Section 3, the blocking time t_b pdf is derived based on considering that the normalized received LiFi-signal power follows a Rayleigh distribution with a scale parameter (σ) that is related to users' density within the LiFi cell.

B. Opportunistic Offloading

The average duration for the opportunistic offloading times based on the timing diagram in Fig. 1(b) are given by

$$\bar{T}_{o(\mathrm{i})} = 0, \tag{14}$$

$$\bar{T}_{o(\mathrm{ii})} = \int_0^{\infty}\int_{t_v=t_b}^{\infty}\int_0^{\infty}\int_{t_r}^{t_r+t_v-t_b}(t_d - t_r - t_b) \times f_{t_d}(t_d) f_{t_r}(t_r) f_{t_v}(t_v) f_{t_b}(t_b)\mathrm{d}t_d\mathrm{d}t_r\mathrm{d}t_v\mathrm{d}t_b, \tag{15}$$

$$\bar{T}_{o(\mathrm{iii})} = \int_0^{\infty}\int_{t_b}^{t_d-t_r}\int_0^{\infty}\int_{t_r+t_v-t_b}^{\infty}(t_v - t_b) \times f_{t_d}(t_d) f_{t_r}(t_r) f_{t_v}(t_v) f_{t_b}(t_b)\mathrm{d}t_d\mathrm{d}t_r\mathrm{d}t_v\mathrm{d}t_b. \tag{16}$$

C. Delayed Offloading

The average duration for the delayed offloading for the timing diagram in Fig. 2(b) are given by

$$\bar{T}_{d(\mathrm{i})} = 0, \tag{17}$$

$$\bar{T}_{d(\mathrm{ii})} = \int_0^{d}\int_{t_b}^{\infty}\int_D^{\infty}\int_{t_r-D}^{t_r+t_v-t_b-D}(t_d + D - t_r - t_b) \times f_{t_d}(t_d) f_{t_r}(t_r) f_{t_v}(t_v) f_{t_b}(t_b)\mathrm{d}t_d\mathrm{d}t_r\mathrm{d}t_v\mathrm{d}t_b, \tag{18}$$

$$\bar{T}_{d(\mathrm{iii})} = \int_0^{d}\int_{t_b}^{\infty}\int_D^{\infty}\int_{t_r+t_v-D-t_b}^{\infty}(t_v - t_b) \times f_{t_d}(t_d) f_{t_r}(t_r) f_{t_v}(t_v) f_{t_b}(t_b)\mathrm{d}t_d\mathrm{d}t_r\mathrm{d}t_v\mathrm{d}t_b, \tag{19}$$

$$\bar{T}_{d(\mathrm{iv})} = \int_0^{d}\int_{t_b}^{\infty}\int_0^{D}\int_0^{t_v-t_b}(t_d - t_b) \times f_{t_d}(t_d) f_{t_r}(t_r) f_{t_v}(t_v) f_{t_b}(t_b)\mathrm{d}t_d\mathrm{d}t_r\mathrm{d}t_v\mathrm{d}t_b, \tag{20}$$

$$\bar{T}_{d(\mathrm{v})} = \int_0^{d}\int_{t_b}^{\infty}\int_0^{D}\int_{t_v-t_b}^{\infty}(t_v - t_b) \times f_{t_d}(t_d) f_{t_r}(t_r) f_{t_v}(t_v) f_{t_b}(t_b)\mathrm{d}t_d\mathrm{d}t_r\mathrm{d}t_v\mathrm{d}t_b. \tag{21}$$

5. RESULTS AND DISCUSSION

We use MATLAB to simulate both opportunistic and delayed scenarios. The simulation is based on event-driven simulation, where random values are generated to all t_r, t_v, t_d, and t_b based on their distributions, state diagram, and timing diagram shown in Figs. 1 and 2. We use the following parameters values: $\mu_v = 100$, $\mu_d = \mu_v/10$, and ratio of LiFi data rate to cellular data rate follows nominal offloading rates $R_v : R_C = 5 : 2$ [29]. The threshold minimum power Γ_{TH} is assumed to be 50% of the LiFi transmitted power.

Figures 5(a) and 5(b) show offloading efficiency in the case of the opportunistic scenario with and without LiFi blocking, respectively. The offloading efficiency is shown versus the mean of cellular residence time normalized by the mean of LiFi residence time considering. Figure 5(a) shows the two cases of blocking and non-blocking at different values of the variability parameter ($a = 1$, 3, and 5) and at a scale parameter value of $\sigma = 1.33$. It is clear that LiFi-signal blocking reduces the amount of offloaded traffic from the cellular network by more than 30%. Concerning the effect of changing the variability parameter a for the non-blocking case, as a increases, the offloading efficiency decreases. This can be explained as follows. Increasing a leads to more skewing toward the left with a longer tail of the distribution. This means a smaller LiFi residence time, which results in most of the traffic carried by the cellular network. In the case of LiFi-signal blocking, the effect of changing a is reversed. It can be explained as follows. Reducing a results in less skewing toward the left with a shorter tail of the distribution. This means a higher LiFi residence time. Consequently, this leads to higher probability of LiFi-signal blocking, and the overall offloading efficiency is reduced.

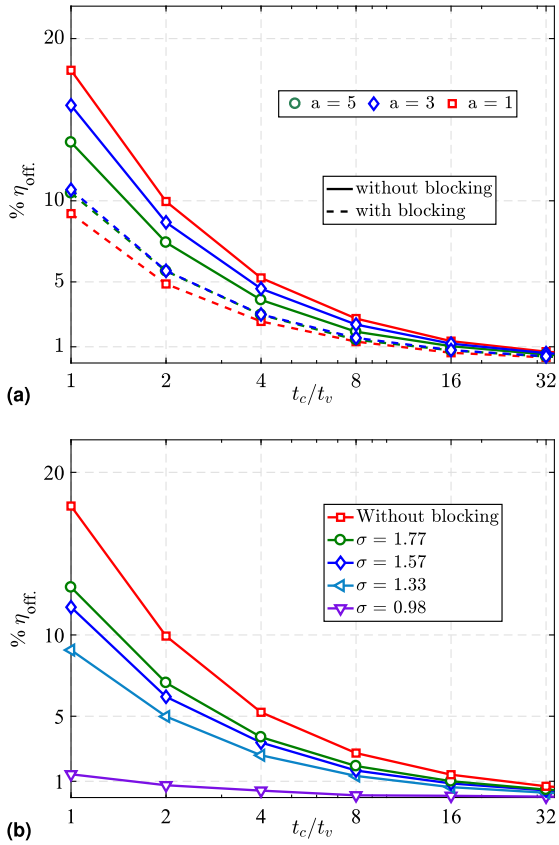

Fig. 5. Offloading efficiency (η_{off}) versus the ratio t_c/t_v at (a) different values of variability parameter ($a = 1$, 3, 5) for opportunistic scenario with and without LiFi blocking; (b) different levels of users' density ($\sigma = 1.77$, 1.33, 1.57, 0.98) at a variability parameter of $a = 1$, taking LiFi-signal blocking.

Figure 5(b) illustrates the effect of users' density within the LiFi cell on the offloading efficiency. The offloading efficiency is drawn versus the mean of cellular residence time normalized by the mean of LiFi residence time at different values of scale parameter σ. It is found that, by increasing the users' density (decreasing σ), the shadowing effect increases. Hence, the

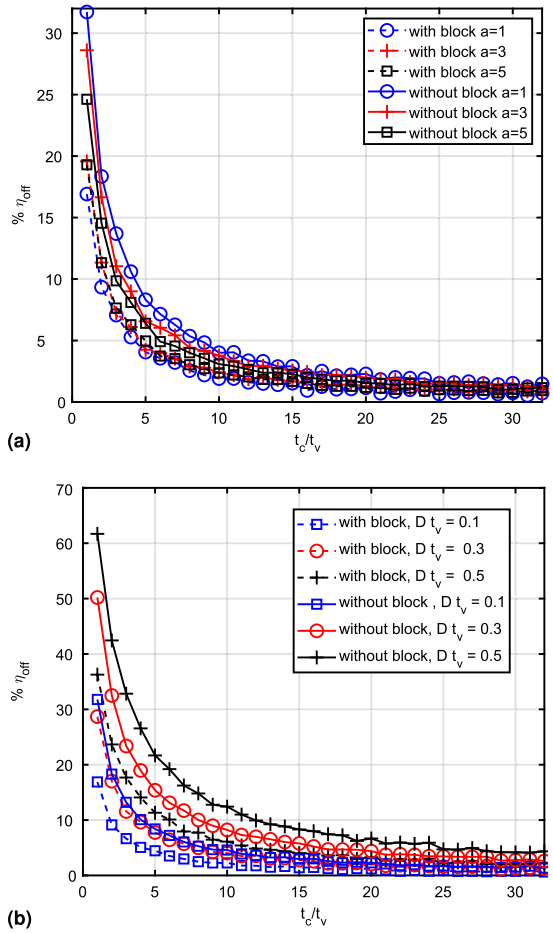

Fig. 6. Offloading efficiency (η_{off}) versus the ratio t_c/t_v at (a) different values for delayed offloading scenario of variability parameter ($a = 1, 3, 5$) with and without LiFi blocking; (b) different delayed timings are represented as a ratio of t_v level considering several users' density of ($\sigma = 0.1, 0.3, 0.5$) with and without LiFi blocking.

blocking probability increases, and consequently the offloading efficiency decreases.

Figure 6 shows the offloading efficiency versus the mean of cellular residence time normalized by the mean of LiFi residence time for the delayed scenario. We considered the effects of factor a, delay time D, and blocking on offloading efficiency. In Fig. 6(a), the effect of changing variability parameter a is illustrated for the delayed case for $D = 0.1/t_v$. The same conclusion given about effect of variable parameter a in Fig. 5(a) holds here in Fig. 6(a). In addition, comparing results in Fig. 6(a) with that given in Fig. 5(a) illustrates the improvement in offloading efficiency by using the delayed scenario. For example, offloading efficiency increases from 18% in the opportunistic scenario with $a = 1$ and no blockage to 32% in the case of the delayed scenario under the same conditions. However, due to the delay in starting the communication process in the case of delayed offloading, mobile operators should apply an incentive system, i.e., decrease cost per gigabyte, to motivate mobile users to wait for some time while searching for LiFi coverage.

In Fig. 6(b), the effect of delay time D is investigated. It is clear that increasing D leads to an increase in the offloading efficiency because the user can wait more until the user finds a LiFi AP. Specifically, with no blockage, offloading efficiencies of 32%, 50%, and 62% are achieved with $D = 0.1/t_v$, $D = 0.3/t_v$, and $D = 0.5/t_v$, respectively. Accordingly, the offloading efficiency of the delayed scenario is enhanced by at least 40%, when compared with the opportunistic scenario, in most of the cases. In case of blockage, offloading efficiencies of 18%, 30%, and 38% are achieved for the same values of delay times.

6. CONCLUSION

Future information-hungry applications are anticipated to experience congestion in HetNets, particularly cellular networks. It is particularly important to employ cellular/LiFi offloading schemes so that LiFi can carry some data traffic from cellular networks. We have investigated the traffic offloading efficiency of the cellular/LiFi HetNet. A framework of opportunistic and delayed cellular/LiFi offloading and temporal order diagrams for various disjoint cases are illustrated. Statistical distributions for different times have been given for realistic scenarios. In addition, the offloading efficiency of the delayed scenario is improved by at least 40%, when compared with the opportunistic case, in most of the cases. Our results reveal that in dynamic channels LiFi blocking reduces traffic offloading efficiency. The dynamic VLC channel blockage time is modeled by Rayleigh distribution based on the results of simulation using the Zemax solver.

Disclosures. The authors declare no conflicts of interest.

Data Availability. Data underlying the results presented in this paper are not publicly available at this time but may be obtained from the authors upon reasonable request.

REFERENCES

1. "Cisco Visual Networking Index: Global Mobile Data Traffic Forecast Update (2016-2021)," White Paper, 2021,https://www.cisco.com/c/en/us/solutions/collateral/executive-perspectives/annual-internet-report/white-paper-c11-741490.html.
2. N. Al-Falahy and O. Alani, "Millimeter wave frequency band as a candidate spectrum for 5G network architecture: a survey," Phys. Commun. **32**, 120–144 (2018).
3. H. Haas, "LiFi is a paradigm-shifting 5G technology," Rev. Phys. **3**, 26–31 (2017).
4. F. Rebecchi, M. D. de Amorim, V. Conan, A. Passarella, R. Bruno, and M. Conti, "Data offloading techniques in cellular networks: a survey," Commun. Surveys Tuts. **17**, 580–603 (2015).
5. Y. He, M. Chen, B. Ge, and M. Guizani, "On Wifi offloading in heterogeneous networks: various incentives and trade-off strategies," Commun. Surveys Tuts. **18**, 466–490 (2016).
6. Y. Niu, Y. Li, D. Jin, L. Su, and A. V. Vasilakos, "A survey of millimeter wave communications (mmWave) for 5G: opportunities and challenges," Wireless Netw. **21**, 2657–2676 (2015).
7. B. Liu, Q. Zhu, W. Tan, and H. Zhu, "Congestion-optimal WiFi offloading with user mobility management in smart communications," Wireless Commun. Mob. Comput. **2018**, 9297536 (2018).
8. N. Wahab, A. Isa, M. Ahmad, and R. Ruliyanta, "Augmenting mobile data networks using WiFi offloading: a measurement study," J. Telecommun. Electron. Comput. Eng. **10**, 119–123 (2018).
9. D. Suh, H. Ko, and S. Pack, "Efficiency analysis of WiFi offloading techniques," IEEE Trans. Veh. Technol. **65**, 3813–3817 (2016).
10. H. Haas, L. Yin, Y. Wang, and C. Chen, "What is LiFi?" J. Lightwave Technol. **34**, 1533–1544 (2016).

11. M. Kashef, M. Abdallah, K. Qaraqe, H. Haas, and M. Uysal, "Coordinated interference management for visible light communication systems," J. Opt. Commun. Netw. **7**, 1098–1108 (2015).
12. S. Wu, H. Wang, and C. H. Youn, "Visible light communications for 5G wireless networking systems: from fixed to mobile communications," IEEE Netw. **28**, 41–45 (2014).
13. M. Z. Afgani, H. Haas, H. Elgala, and D. Knipp, "Visible light communication using OFDM," in *2nd International Conference on Testbeds and Research Infrastructures for the Development of Networks and Communities* (2006), pp. 6–134.
14. M. Ayyash, H. Elgala, A. Khreishah, V. Jungnickel, T. Little, S. Shao, M. Rahaim, D. Schulz, J. Hilt, and R. Freund, "Coexistence of WiFi and LiFi toward 5G: concepts, opportunities, and challenges," IEEE Commun. Mag. **54**(2), 64–71 (2016).
15. A. Al-Kinani, C. Wang, L. Zhou, and W. Zhang, "Optical wireless communication channel measurements and models," Commun. Surveys Tuts. **20**, 1939–1962 (2018).
16. A. E. Elfiqi, H. S. Khallaf, S. F. Hegazy, A. Elsonbaty, H. M. H. Shalaby, and S. A. Obayya, "Chaotic polarization-assisted *L* DPSK-MPPM modulation for free-space optical communications," IEEE Trans. Wireless Commun. **18**, 4225–4237 (2019).
17. H. S. Khallaf and M. Uysal, "UAV-based FSO communications for high speed train backhauling," in *IEEE Wireless Communications and Networking Conference (WCNC)* (2019), pp. 1–6.
18. E. Sarbazi, M. Uysal, M. Abdallah, and K. Qaraqe, "Indoor channel modelling and characterization for visible light communications," in *16th International Conference on Transparent Optical Networks (ICTON)* (2014), pp. 1–4.
19. F. Miramirkhani and M. Uysal, "Channel modeling and characterization for visible light communications," IEEE Photon. J. **7**, 1–16 (2015).
20. P. Chvojka, S. Zvanovec, P. A. Haigh, and Z. Ghassemlooy, "Channel characteristics of visible light communications within dynamic indoor environment," J. Lightwave Technol. **33**, 1719–1725 (2015).
21. A. E.-R. A. El-Fikky, M. E. Eldin, H. A. Fayed, A. A. El Aziz, H. M. Shalaby, and M. H. Aly, "NLoS underwater VLC system performance: static and dynamic channel modeling," Appl. Opt. **58**, 8272–8281 (2019).
22. A. E.-R. A. El-Fikky, A. S. Ghazy, H. S. Khallaf, E. M. Mohamed, H. M. Shalaby, and M. H. Aly, "On the performance of adaptive hybrid MQAM–MPPM scheme over Nakagami and log-normal dynamic visible light communication channels," Appl. Opt. **59**, 1896–1906 (2020).
23. F. Miramirkhani, O. Narmanlioglu, M. Uysal, and E. Panayirci, "A mobile channel model for VLC and application to adaptive system design," IEEE Commun. Lett. **21**, 1035–1038 (2017).
24. H. S. Khallaf, A. E. El-Fiqi, M. Elwekeil, H. M. H. Shalaby, and S. S. A. Obayya, "Efficiency of opportunistic cellular/LiFi traffic offloading," in *19th International Conference on Transparent Optical Networks (ICTON)* (2017), pp. 1–4.
25. Behlouli, P. Combeau, S. Sahuguède, A. Julien-Vergonjanne, C. Le Bas, and L. Aveneau, "Impact of physical and geometrical parameters on visible light communication links," in *Advances in Wireless and Optical Communications (RTUWO)* (2017), pp. 73–76.
26. "Grab CAD models," 2018, https://grabcad.com.
27. "Zemax programming language," 2018, https://customers.zemax.com/os/resources/learn/knowledgebase/what-is-zpl.
28. Y. Fang, I. Chlamtac, and Y.-B. Lin, "Channel occupancy times and handoff rate for mobile computing and PCS networks," IEEE Trans. Comput. **47**, 679–692 (1998).
29. K. Lee, J. Lee, Y. Yi, I. Rhee, and S. Chong, "Mobile data offloading: how much can WiFi deliver?" IEEE/ACM Trans. Netw. **21**, 536–550 (2013).